



## Introduction

A non-resonant divertor system is being designed for the Eos quasi-axisymmetric stellarator. Research into magnetic field topology, system power balance calculations, and development of boron pebble extrusions to accommodate high heat and particle fluxes in the exhaust region are outlined.

## Magnetic Field Calculations and Flux Surface Poincare Plots

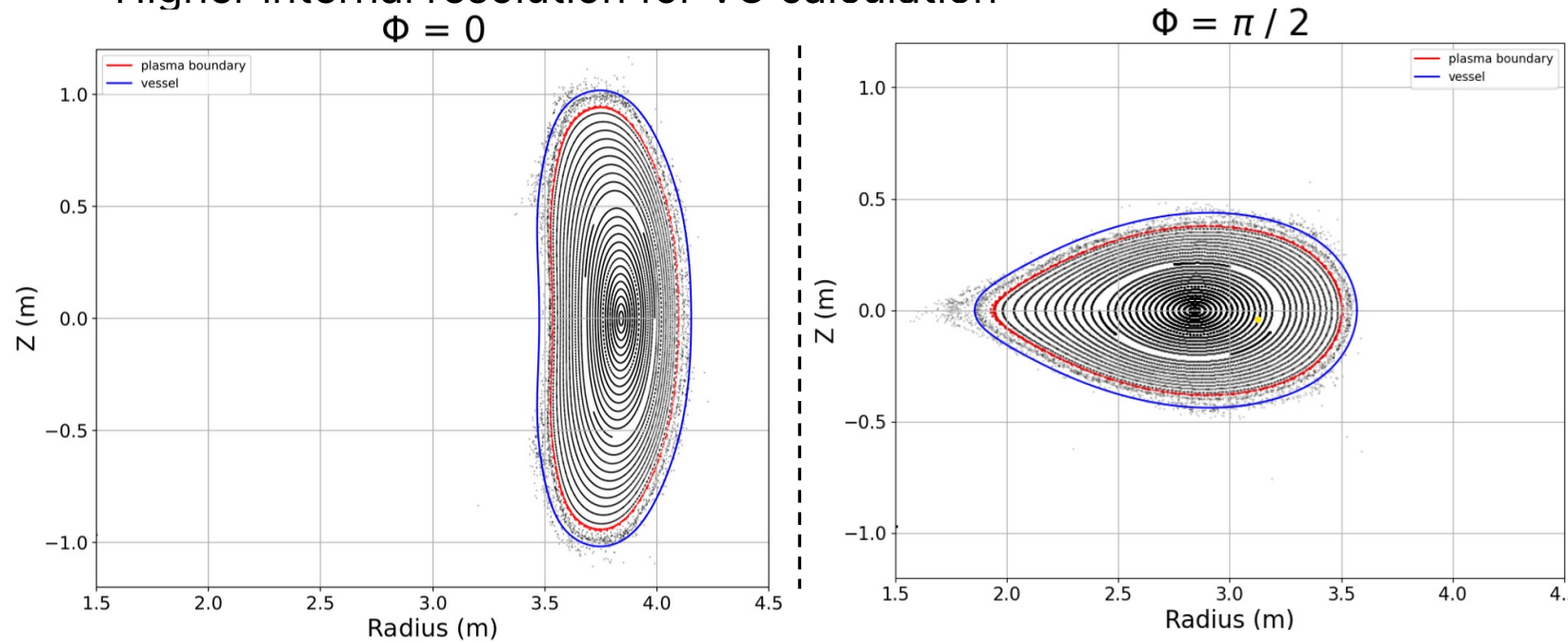
We use the FIELDLINES<sup>[1]</sup> module in the STELLOPT code suite to calculate total magnetic field of our equilibrium, after validating the code on HSX data<sup>[2]</sup>.

- Internal to the plasma boundary, the equilibrium plasma field is applied, to maintain ideal closed nested flux surfaces.<sup>[3]</sup>
- External magnetic field external is calculated from the plasma response and coil fields using the virtual casing (VC) principle, extended from the boundary.
- To maintain accuracy near the surface of the plasma, the VC principle employs an adaptive integration scheme over the surface current.

Once total magnetic field is calculated, FIELDLINES executes field line tracing following, allowing us to evaluate flux surface quality via Poincare plots.

Several factors improved the flux surface quality:

- Vacuum magnetic field accuracy via direct Biot-Savart field calculations or higher resolution magnetic grids
- Higher nested surface resolution within the equilibrium
- Higher internal resolution for VC calculation



Plots of FIELDLINES code field line tracing results at two toroidal Poincare sections, to illustrate flux surfaces in the plasma core and edge. The two plots are at the "bean" (left) and "teardrop" (right) toroidal cross-sections. The plasma boundary is plotted in red, and a 5 cm plasma offset for a potential first wall location is plotted in blue, over the FIELDLINES tracing results.

- Ideal nested flux surfaces transition at the edge to open field lines.
- The last closed flux surface (LCFS) is estimated to be near the plasma boundary, and qualitatively evaluated in these plots.
- For our base case equilibrium, LCFS is slightly within the plasma boundary.

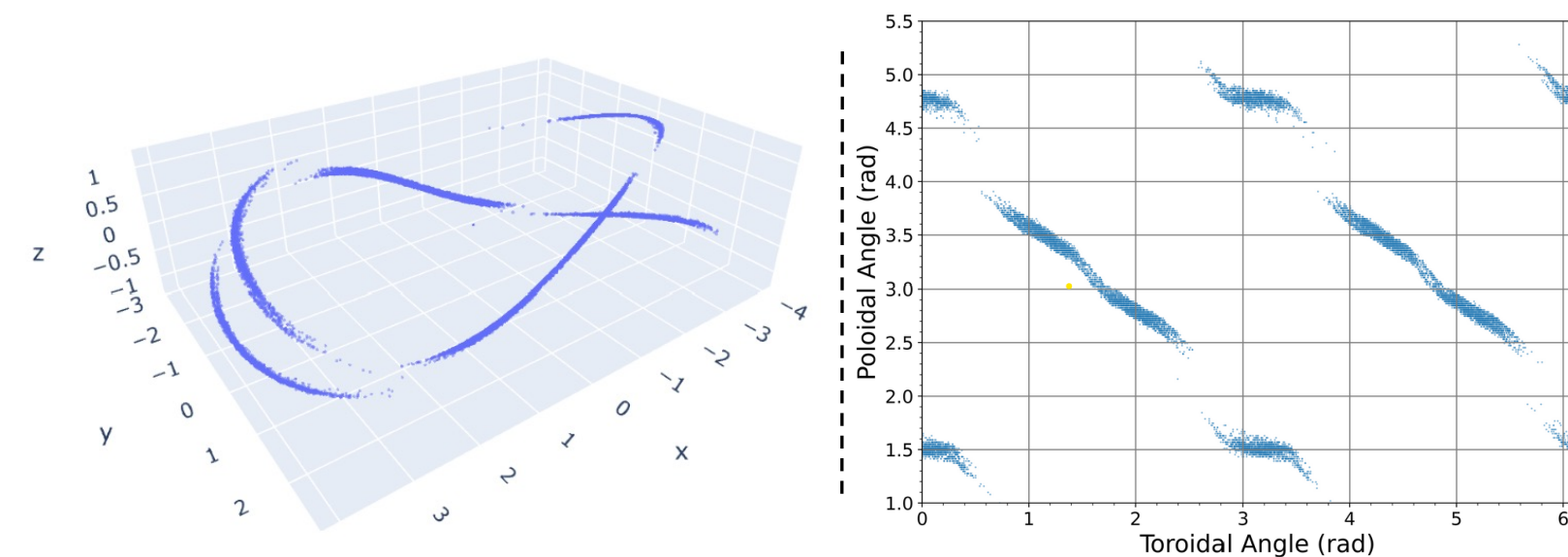
## Field Line Tracing

Two codes, STELLOPT FIELDLINES and DIV3D (ORNL)<sup>[4]</sup> perform field line tracing incorporating diffusion to:

- approximate particle trajectories beyond the last closed flux surface,
- illustrate exhaust locations via strike points on an offset vessel.

We conduct a study on strike point resilience using these tracing tools, with respect to vessel wall offset and diffusion coefficient.

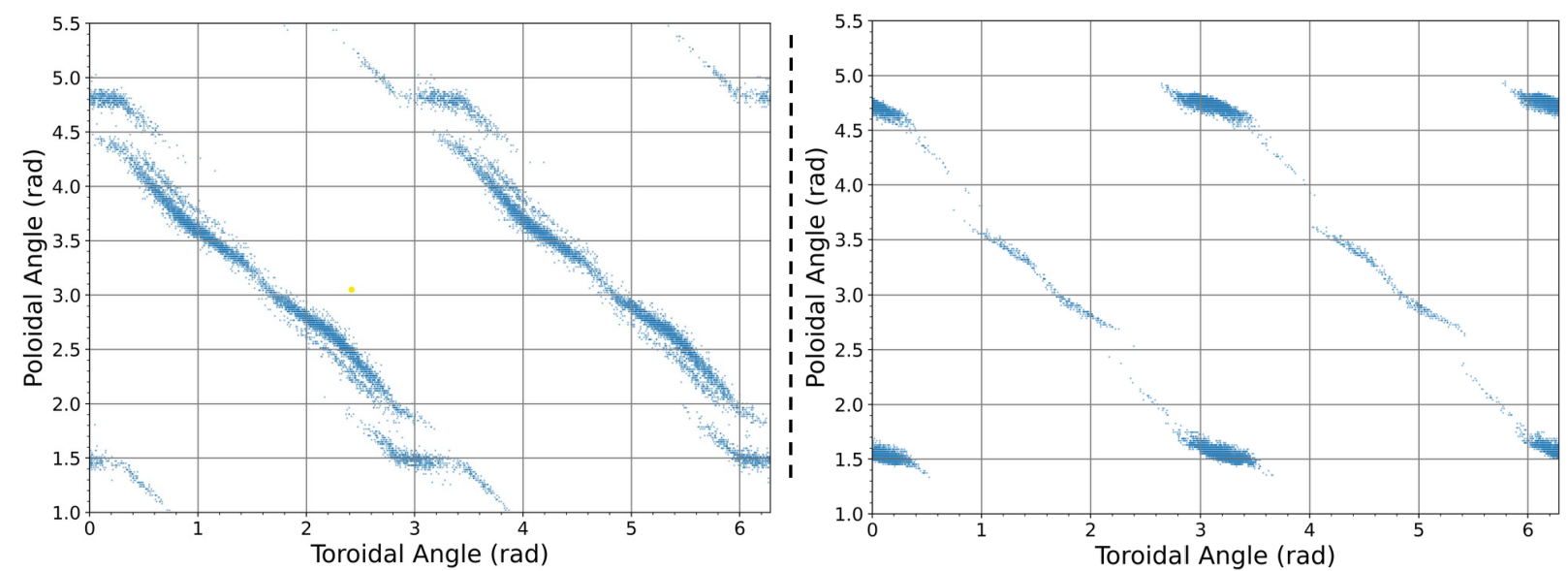
### BASE CASE EQUILIBRIUM STRIKE POINTS:



3D plot of strike points from field lines traced from the plasma LCFS, as they intersect with a 5 cm offset vessel. Diffusion coefficient of  $10^{-7} \text{ m}^2 / \text{m}$ .

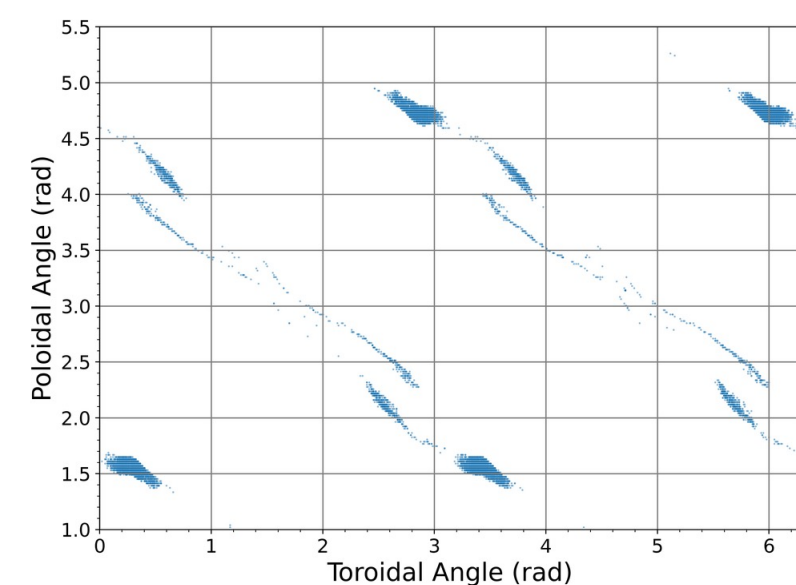
2D plot of strike points, translated from (x,y,z) to toroidal-poloidal coordinates via a length-normalized mapping.

### WALL OFFSET SCAN

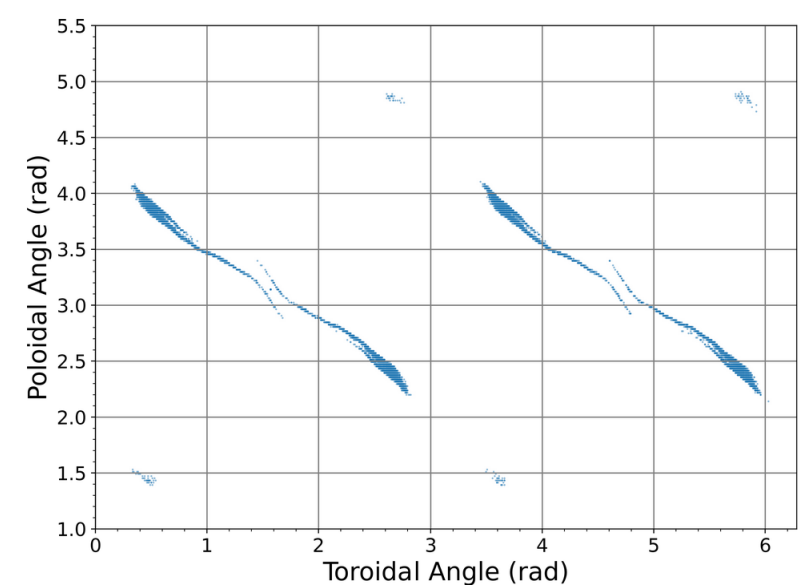


Tor-pol plot of strike points at wall offset of 2.5 cm.

Tor-pol plot of strike points at wall offset of 7.5 cm.



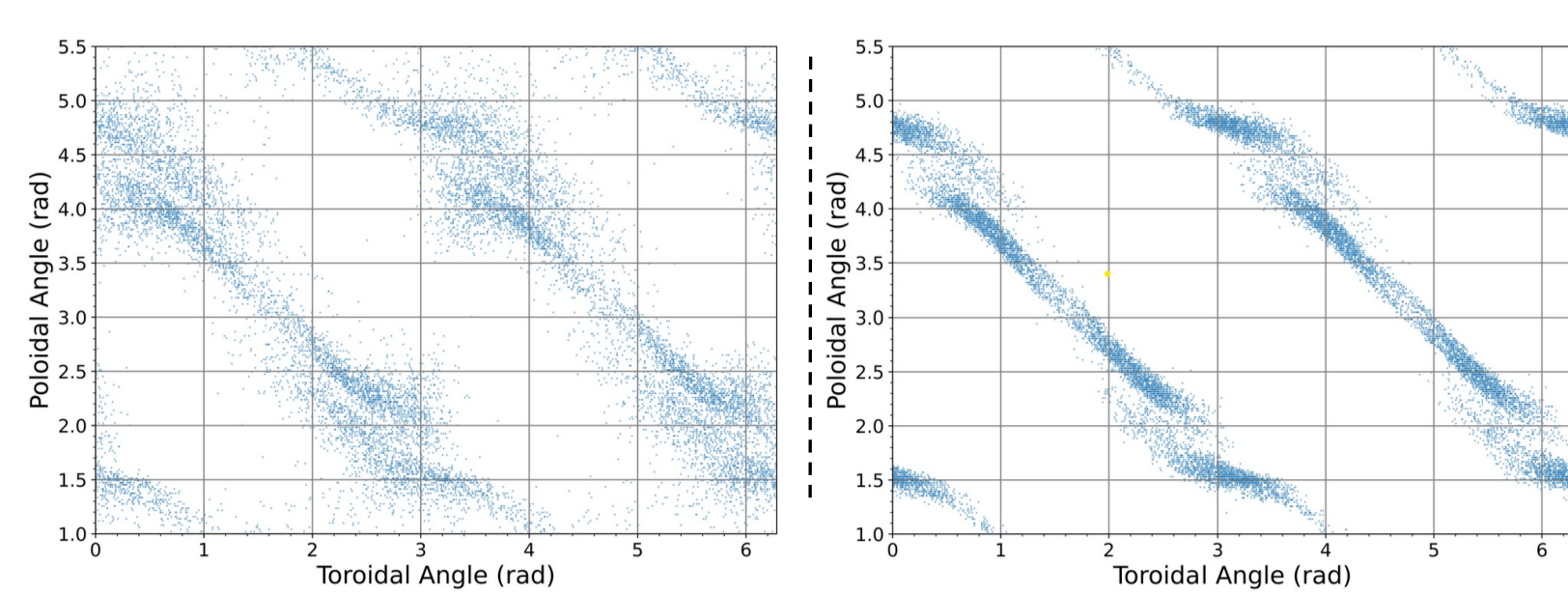
Tor-pol plot of strike points at wall offset of 10 cm.



Tor-pol plot of strike points at wall offset of 12.5 cm.

- Strike points lie in helical lines along regions of peak curvature.
- Aligns with Boozer's hypothesis<sup>[5]</sup> that plasma flux preferentially leaves through the LCFS from regions of high curvature, due to geometrical and flux expansion arguments.
- The wall offset defines the space the particles have to traverse the stellarator and radiate energy.
- As it increases, the strike point pattern concentrates in toroidally distinct locations, though remain within regions of high curvature.

### DIFFUSION COEFFICIENT SCAN



Tor-pol plot of strike points, diffusion  $10^{-5} \text{ m}^2 / \text{m}$ .

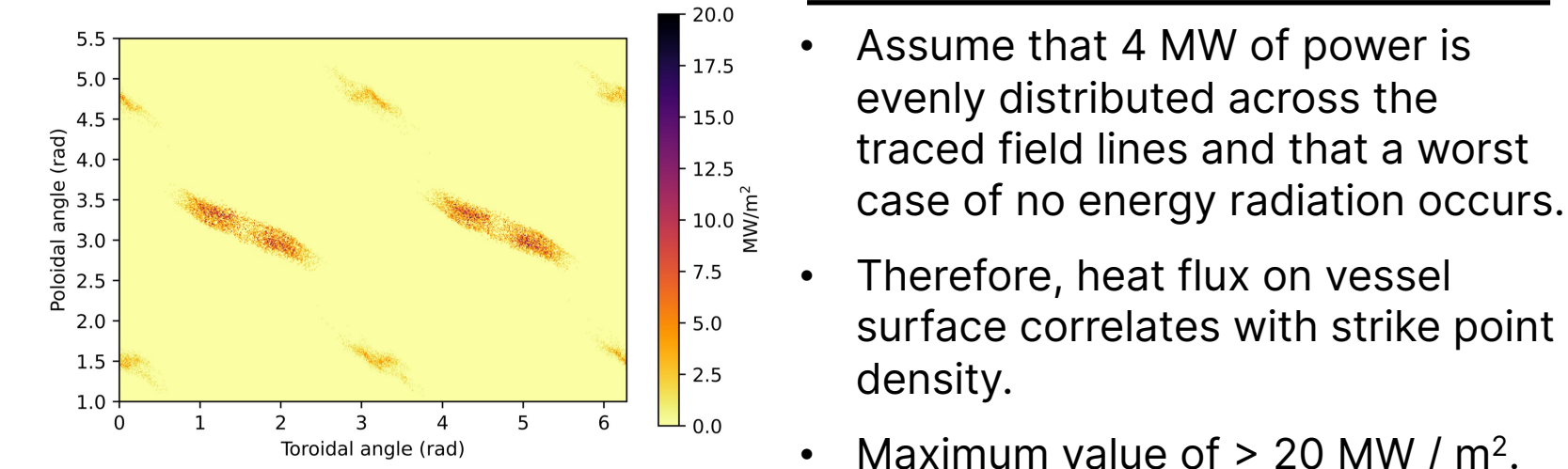
Tor-pol plot of strike points, diffusion  $10^{-6} \text{ m}^2 / \text{m}$ .

- The diffusion coefficient value determines amount of perpendicular diffusion by particles as they follow field lines.
- As it approaches zero, particles follow field lines more closely and the strike points become more concentrated into helical patterns, localizing heat flux.

## Heat Flux Calculations

- The total power incident on the divertor is estimated to be 4 MW.<sup>[6]</sup>
- 20% of neutral beam power falls on the beam dump via shine-through.
- Remaining power is split 50% to first wall and 50% to divertor.

Table 1 – Eos Power Flows		
Variable	Value	Units
Incident beam power	10	MW
Shine-through power	2	MW
Power incident on first wall	4	MW
Power incident on divertor	4	MW



- Assume that 4 MW of power is evenly distributed across the traced field lines and that a worst case of no energy radiation occurs.
- Therefore, heat flux on vessel surface correlates with strike point density.
- Maximum value of  $> 20 \text{ MW} / \text{m}^2$ .

## Renewable Boron Pebble Extrusion System

We explore a conceptual design for a renewable pebble system with boron plasma-facing surfaces, in partnership with UCSD via an INFUSE grant.

$$\dot{m} = \frac{P * M}{\Delta H_{vap}}$$

The worst case mass flow rate of boron needed to capture 4 MW of heat using the material heat of vaporization is **81 g / s** which is impractically high.

$$\dot{m} = \frac{m_w \sum Y_i x_i P_{DIV}}{N_{AV} 2q_e V}$$

A sputtering calculation<sup>[7]</sup> via the yield for D and He on a boron target suggests a mass replenishment rate of **0.036 g / s**.

- UCSD has developed boron pebble rods using a boron nitride binding matrix.
- Key boron performance metrics are tested on the heat flux test stand, where a laser directs up to 40 MW / m<sup>2</sup> of heat flux onto the test specimen.
- Diagnostic systems measured minimal erosion and outgassing, and a surface temperature of up to 2400 K.
- The PISCES-A linear plasma device simulates a divertor plasma (H or He) with smaller heat flux ( $\sim 0.5 \text{ MW} / \text{m}^2$ ), for long periods of exposure.
- They measure heating (visible and IR imaging), sputtering (visible spectroscopy), and hydrogen retention (thermal desorption spectroscopy).



## Conclusion

Key research objectives are met in the path to developing a conceptual non-resonant divertor design. In carrying out the magnetic field topology analysis and heat flux evaluation, we are prepared to start iterating on divertor positioning, geometry, and surface optimizations. Initial investigation of renewable boron geometries as plasma-facing surfaces shows promise (see UCSD poster for full results). Future work includes higher fidelity plasma edge modelling, further PMI experimentation, calculating pumping needs, and simulating operational regimes.

## References

1. S. A. Lazerson et al., "First measurements of error fields on W7-X using flux surface mapping," *Nucl. Fusion*, vol. 56, no. 10, p. 106005, (Oct. 2016).
2. A. Bader et al., "HSX as an Example of a Resilient Non-Resonant Divertor," *Physics of Plasmas* 24, no. 3, (March 1, 2017): 032506.
3. S. A. Lazerson et al. (n.d.). ["STELLOPT"]. <https://princetonuniversity.github.io/STELLOPT/FIELDLINES>
4. J. D. Lore, et al., "Design and Analysis of Divertor Scraper Elements for the W7-X Stellarator," *IEEE Transactions on Plasma Science*, vol. 42, no. 3, (Mar. 2014): 539–544.
5. A. H. Boozer, "Stellarator design," *J. Plasma Phys.* 81, 515810606, (2015).
6. J. F. Lyon et al., "Systems Studies and Optimization of the ARIES-CS Power Plant," *Fusion Science and Technology* vol. 54, no. 3, (October 2008): 694–724.
7. G.M. Voss et al., "The Cascading Pebble Divertor for the Spherical Tokamak Power Plant," *Fusion Engineering and Design* 81, no. 1–7 (2006): 327–333.